

Initiation Dynamics of Rotating Detonation Engines using $C_2H_4-O_2$ Mixtures

Sean F. Connolly-Boutin¹, Mohammad Ghali², Ritchard Gilot², Jason Loiseau³,
Andrew J. Higgins², Charles B. Kiyanda¹

¹Concordia University
Department of Mechanical, Industrial and Aerospace Engineering
Montreal, Quebec, Canada

²McGill University
Department of Mechanical Engineering
Montreal, Quebec, Canada

³Royal Military College
Department of Chemistry and Chemical Engineering
Kingston, Ontario, Canada

1 Introduction

The last 20 years have seen a renewed interest for the rotating detonation engine (RDE) concept, consisting of an annular combustion chamber continuously filled with a detonable fuel-oxidizer mixture at one end. One or more detonation waves travel circumferentially, either co-rotating in the same direction at comparable and roughly steady speeds, or counter-rotating in opposite directions, leading to periodic collision-extinction-reignition events. The initial work of Bykovskii, Zhdan, and others [1–3] laid the groundwork for the dynamics of detonation waves propagating in continuous-like, azimuthal directions, but in pre-filled geometries. An extensive body of work has been rapidly developing examining the steady-state operation of RDEs, their operating modes and instabilities (see e.g. [4–7]). However, while the dynamics and stability of the engines are being extensively investigated in the self-sustained operating regime, the initial transient dynamics that lead to the establishment of a self-sustained flow field are still poorly understood, and few publications examine the issue specifically. Owing to their simplicity, physical robustness, and repeatability, pre-detonator tubes are often favoured for the initiation of RDEs. However, the use of a predetonator tube requires: a secondary filling system; depending on the main mixture type, a secondary mixture; and, ideally, isolation from the main chamber before and after initiation would be achieved through diaphragms, timed valves, or an equivalent system. The dynamics of detonation transition from pre-detonator tubes to an operating RDE has been studied experimentally by St. George et al. [8] and numerically by Zheng et al [9]. The difference in initiation dynamics between a predetonator and an automotive-type spark plug is reported by Mizener et al [10].

RDE initiation through low-energy, timed spark discharges were also investigated [11]. More recently, Shehab Elhawary et al. tackled the more fundamental problem of detonation transition into supersonic flow [12].

The development of commercially viable RDE hardware requires an initiation system that can be fired multiple times to re-ignite after an unstart or flameout, a requirement for which electrical initiation is better suited, despite its challenges. In this work, we systematically examine the influence of initiator construction, placement and delivered energy on the transient initiation dynamics of RDEs.

2 Experimental Setup: Engine Geometry, Injection, and Igniter Designs

The RDE geometry tested is a straight, throatless, 5.5 mm height, annular combustion chamber with radial/axial non-premixed injection of C_2H_4/O_2 mixtures. The nominal combustion chamber diameter is 69.9 mm (2.75 in.). Two injector geometries were tested. Both geometries use impinging jets to mix fuel and oxidizer inside the annulus, normally with oxygen flowing axially and fuel flowing radially through the center body. One injector, shown in fig. 1, consists of 24 radial (fuel) injection holes and 40 axial (oxygen) injection holes, all 3.175 mm (1/8 in.) in diameter. The radial injection plane is located 6.35 mm (0.25 in.) downstream of the axial injection plane. The second injector, shown in fig. 2, consists of 62 axial (oxygen) injection holes of 0.79 mm (1/32 in.) diameter, and 42 square, radial (fuel) slots on the center body, each 0.79 mm (1/32 in.) by 0.40 mm (1/64 in.) in size. In this injector geometry, the radial (fuel) injection area is closed by the axial injector plate, such that the radial injectors are as close as possible to the axial injectors.

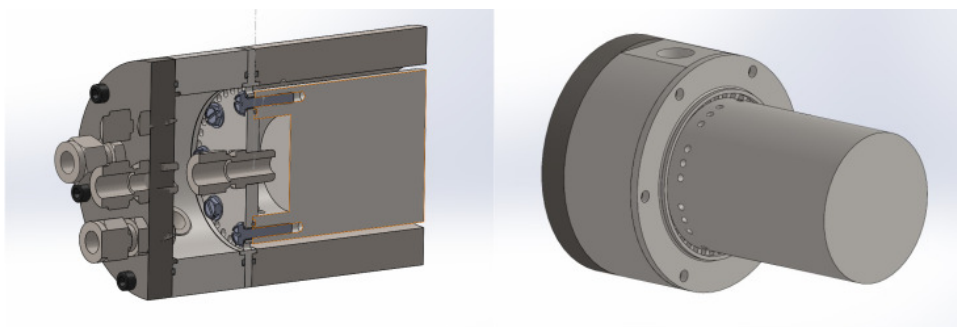


Figure 1: Section view of the RDE with downstream radial injectors. Complete sectioned assembly (left) and solid model with the outer wall of the combustion chamber omitted (right).



Figure 2: Model of the RDE with face injectors shown without the outer combustion chamber wall (left). Note the location of the radial injection slots, along the injector plate surface in the central part (right).

The reactant injection system comprises two independent, unregulated blowdown, injection lines. Each line consists of a collector tank, initially pressurized with 20–70 atm of fuel or oxidizer. The injection is controlled by a solenoid valve and the rate of injection is limited by a precalibrated needle valve. Each line enters a roughly 6.3 m³ blast chamber that houses the RDE, such that no gas can mix outside the protected environment. Pressure transducers are located on each injection line to measure the total pressure in the collector tanks and the static line pressure. Total mass flow rates between 100 and 600 g/s have been tested at a nominally stoichiometric ratio. The wave dynamics could be observed using a Photron SA5 high-speed camera located outside the blast chamber and positioned to observe the self-emitted light from the detonation fronts. Video images were acquired at 75 kfps, yielding an inter-frame time of 13.3 μ s.

Two different electrical ignition systems are used. A low energy (LEI) igniter is based on a commercial, automotive capacitor discharge ignition (CDI) box in conjunction with an ignition coil. The coil is a transformer that converts a 12 V input to produce a 1.2 kV output spark, and the CDI controls the spark discharge. A train of sparks could be produced, with the frequency (200-500 Hz) and duration (10-50 ms) controlled by an Arduino Nano microcontroller. The typical energy deposition from an automotive spark, though dependent on several factors—such as the electrical resistance of the system, and gas pressure—is on the order of 10-30 mJ [13]. The energy deposited by the LEI, depending on frequency and duration, is estimated between 10–1000 mJ, but over a finite, relatively long time.

A high-energy igniter (HEI) is also used and consists of a capacitive spark discharge. A DC-DC converter takes a 14 V input and charges a 0.5 μ Fd capacitor to a voltage varying between 1 and 4.5 kV. The system discharge is controlled by a spark gap, triggered by an auxiliary, high voltage but low-energy spark. The stored energy corresponding to the range of voltages is 0.25–5 J. The electrical discharges are delivered through custom plugs inserted radially in the outer combustion chamber wall. The igniter plugs are held in place by a modified Swagelok ultra-torr fitting (Swagelok SS-4-UT-1-2 or SS-6-UT-1-2) bored to allow passage of the full igniter plug diameter. The outer combustion chamber wall is tapped with a blind hole to accept the ultra-torr fitting and a concentric, smooth-bore hole ensures minimal clearance in the final assembly as well as the possibility of flush insertion of the igniter plug, as shown in fig. 3. The center of the igniter plug is located 7.62 mm (0.3 in.) from the axial injector surface.

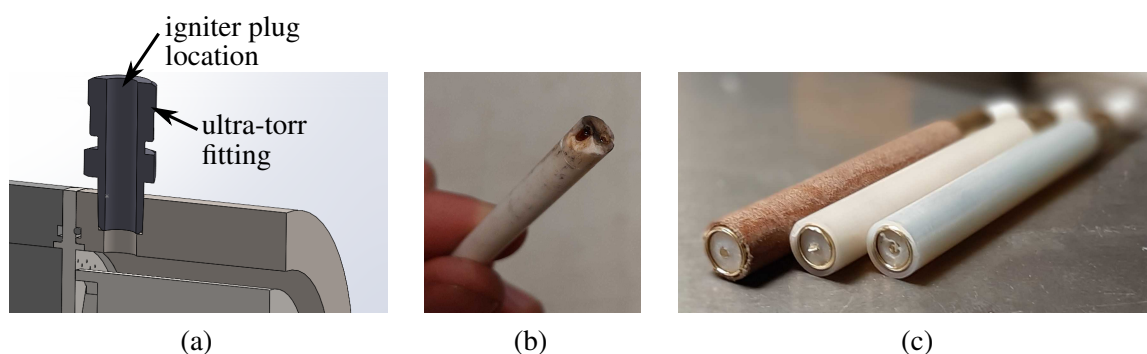


Figure 3: (a) Section view of the igniter plug placement in the outer combustion chamber wall, (b) 2-pin igniter plug (post-firing and showing erosion damage to the insulating ceramic casing after several experiments), and (c) concentric igniter plugs with (left to right) garolite, delrin and nylon external insulators. A concentric igniter with a ceramic insulator was also constructed. (Not shown.)

Two types of plugs have been designed from off-the-shelf materials. The 2-pin plug, fig. 3(b), consists of two parallel, metal pins inserted in a ceramic housing with two through holes. The concentric plug, fig. 3(c), has a tubular brass cathode surrounding a copper anode. Electrical insulation of the concentric

plug is achieved through careful selection of ceramic and plastic tubes that have matching inner and outer dimensions. Each plug could be used for several experiments before needing to be reground to stay flush with the combustion chamber walls. An arduino uno microcontroller controls the timing of injection, initiation, and diagnostic triggering. After the solenoid valve opening, a 100 ms delay allows the injection flow to stabilize, at which point the igniter signal is relayed to the HEI or LEI. The total test duration was limited to 500 ms to limit the overpressurization of the blast chamber.

3 Preliminary Results

The transient, initiation dynamics is, as expected, dependent on the spark energy. Using the HEI, two detonations travelling in opposite directions around the RDE's annulus are generated, as shown in fig. 4. The injector geometry used is that shown in fig. 2, but similar behaviour was observed in both geometries. An obvious, direct initiation, e.g. as would occur from a strong blast decaying smoothly to a detonation, was however not observed. Following the initial spark (top, left frame), a period of $70 \mu\text{s}$ is observed during which no light is emitted. A rapid ignition then occurs at the 7 o'clock position (6th frame), leading to a wave collision at the 3 o'clock position (8th frame). A bright combustion zone then moves counterclockwise on the top section of the annulus and collides with a combustion region around the 3–4 o'clock position.

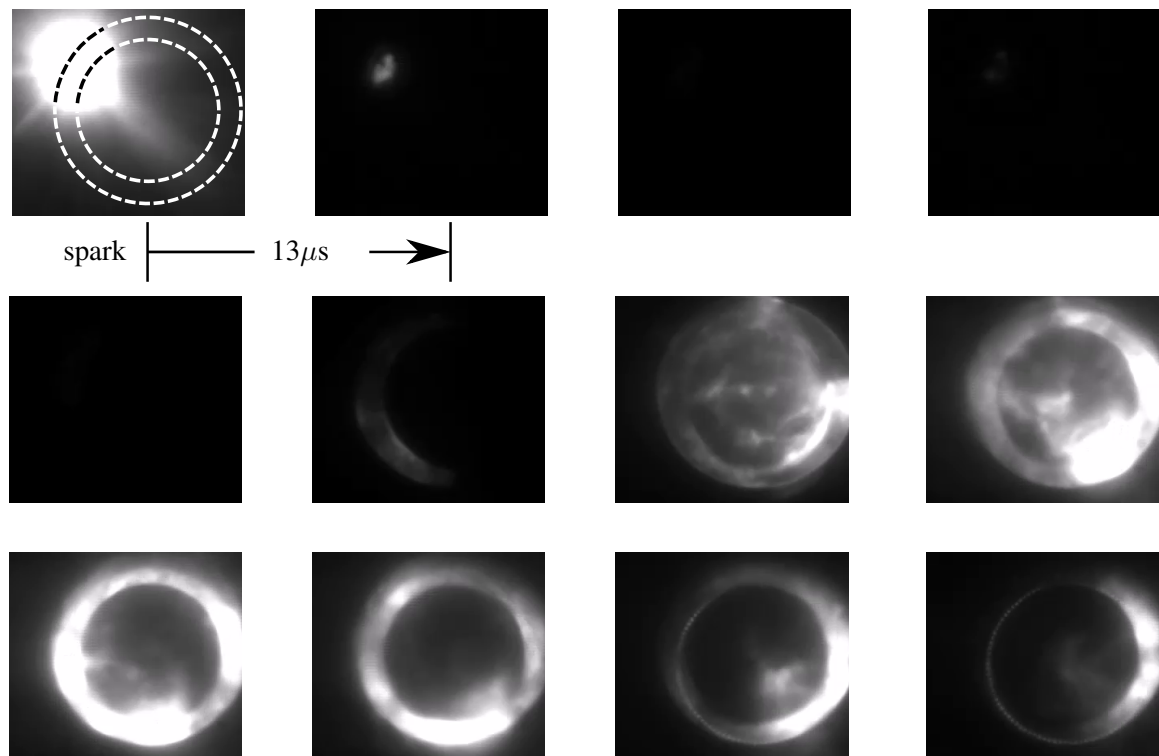


Figure 4: Sequence of frames from initiation using the high-energy igniter, and the 2-pin igniter at a capacitor voltage of 4 kV. Frames are ordered from left to right and top to bottom. In frame 1, the outline of the RDE annulus is indicated by dashed lines. Inter-frame time is a constant $13.3 \mu\text{s}$.

Using the LEI, a much longer initiation delay is observed, as shown in fig. 5. The injector geometry used is that shown in fig. 1. Following the spark discharge (frame 1, top/left), an inactive period of roughly

$770 \mu\text{s}$ is observed. (Frames have been omitted for clarity in fig. 5.) Following this inactive period, a low amount of light is emitted around the 6–8 o'clock position (frames 3 & 4). This region of higher luminosity then travels in the counterclockwise direction as it gains in intensity (frames 5–8). Finally, a region of intense luminosity travels counterclockwise on the bottom of the chamber, although at a speed slower than the CJ velocity.

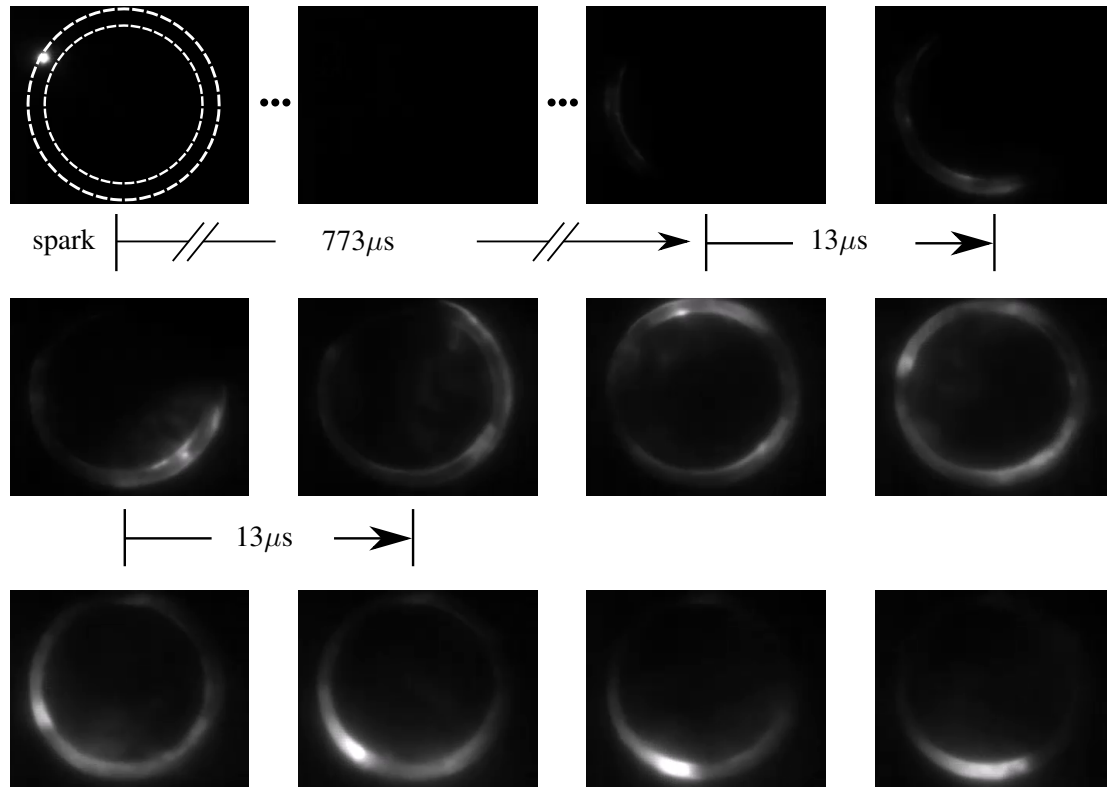


Figure 5: Sequence of frames from initiation using the low-energy igniter, and the 2-pin igniter. Frames are ordered from left to right and top to bottom. In frame 1, the outline of the RDE annulus is indicated by dashed white lines. For conciseness, frames have been omitted during the inactive period, such that the time interval between the first 3 reported frames is $773 \mu\text{s}$. Thereafter, all frames are shown and the inter-frame time is $13.3 \mu\text{s}$.

4 Conclusion

Two different ignition modes have been observed: a rapid ($70 \mu\text{s}$) detonation initiation following a high-energy initiation, resulting in the propagation of counter-rotating waves and their subsequent collision and re-ignition; and a slow ($770 \mu\text{s}$) transition to detonation from a low-energy initiation, resulting in the propagation of a single wave in the counterclockwise direction. Future experiments will incrementally vary the LEI spark train duration and frequencies, the HEI stored energy, the location of the igniter plug with respect to the injection plane, and the injector open areas.

References

- [1] F. A. Bykovskii and V. V. Mitrofanov, "Detonation combustion of a gas mixture in a cylindrical chamber," *Combustion, Explosion, and Shock Waves*, vol. 16, no. 5, pp. 570–578, 1980.
- [2] F. A. Bykovskii, V. V. Mitrofanov, and E. F. Vedernikov, "Continuous detonation combustion of fuel-air mixtures," *Combustion, Explosion and Shock Waves*, vol. 33, no. 3, pp. 344–353, 1997.
- [3] S. A. Zhdan, F. A. Bykovskii, and E. F. Vedernikov, "Mathematical modeling of a rotating detonation wave in a hydrogen-oxygen mixture," *Combustion, explosion, and shock waves*, vol. 43, no. 4, pp. 449–459, 2007.
- [4] V. Anand, A. St. George, R. Driscoll, and E. Gutmark, "Characterization of instabilities in a Rotating Detonation Combustor," *International Journal of Hydrogen Energy*, vol. 40, pp. 16649–16659, Dec. 2015.
- [5] V. Anand, A. St. George, R. Driscoll, and E. Gutmark, "Analysis of air inlet and fuel plenum behavior in a rotating detonation combustor," *Experimental Thermal and Fluid Science*, vol. 70, pp. 408–416, Jan. 2016.
- [6] V. Anand, A. St. George, R. Driscoll, and E. Gutmark, "Longitudinal pulsed detonation instability in a rotating detonation combustor," *Experimental Thermal and Fluid Science*, vol. 77, pp. 212–225, Oct. 2016.
- [7] J. Koch, M. Kurosaka, C. Knowlen, and J. N. Kutz, "Mode-locked rotating detonation waves: Experiments and a model equation," *Physical Review E*, vol. 101, Jan. 2020.
- [8] A. St. George, S. Randall, V. Anand, R. Driscoll, and E. Gutmark, "Characterization of initiator dynamics in a rotating detonation combustor," *Experimental Thermal and Fluid Science*, vol. 72, pp. 171–181, Apr. 2016.
- [9] Y. Zheng, C. Wang, Y. Wang, Y. Liu, and Z. Yan, "Numerical research of rotating detonation initiation processes with different injection patterns," *International Journal of Hydrogen Energy*, vol. 44, pp. 15536–15552, June 2019.
- [10] A. R. Mizener, C. J. Green, and F. K. Lu, "Preliminary Qualitative Observations of Ignition Phenomena in Rotating Detonation Engines," in *22nd AIAA International Space Planes and Hypersonics Systems and Technologies Conference*, (Orlando, FL), American Institute of Aeronautics and Astronautics, Sept. 2018.
- [11] J. A. Boening, J. D. Heath, T. J. Byrd, J. V. Koch, A. T. Mattick, R. E. Breidenthal, C. Knowlen, and M. Kurosaka, "Design and Experiments of a Continuous Rotating Detonation Engine: a Spinning Wave Generator and Modulated Fuel/Oxidizer Mixing," in *52nd AIAA/SAE/ASEE Joint Propulsion Conference*, (Salt Lake City, UT), American Institute of Aeronautics and Astronautics, July 2016.
- [12] S. Elhawary, A. Saat, M. A. Mazlan, and M. A. Wahid, "Ignition Characteristics of Supersonic Combustion," *IOP Conf. Ser.: Mater. Sci. Eng.*, vol. 884, p. 012107, July 2020.
- [13] M. J. Lee, M. Hall, O. A. Ezekoye, and R. D. Matthews, "Voltage, and Energy Deposition Characteristics of Spark Ignition Systems," in *SI Combustion and Direct Injection SI Engine Technology*, pp. 2005–01–0231, Apr. 2005.